

Received October 6, 2020, accepted October 15, 2020, date of publication November 3, 2020, date of current version November 13, 2020.

Digital Object Identifier 10.1109/ACCESS.2020.3035445

Numerical Prediction of DC Breakdown Characteristics in LDPE With Current Profile as Critical Index

MINHEE KIM^{id}, SU-HUN KIM^{id}, (Member, IEEE), AND SE-HEE LEE^{id}

School of Electronic and Electrical Engineering, Kyungpook National University, Daegu 41566, South Korea

Corresponding author: Se-Hee Lee (shlees@knu.ac.kr)

This work was supported in part by Korea Electric Power Research Institute (KEPRI) under Grant BS123456, and in part by the National Research Foundation of Korea (NRF) grant funded by the Korea Government [Ministry of Science and ICT (MSIT)] under Grant 2020R1A2C2013311.

ABSTRACT Understanding the DC breakdown characteristics of polymeric insulators is essential for stable operation of high-capacity DC electrical equipment. To predict the breakdown characteristics of low-density polyethylene (LDPE), we propose a numerical methodology with a new critical index in which the internal current varying with temperature, thickness, and injection barrier height. To evaluate this current-based index, we applied the fully coupled bipolar charge transport (BCT) and molecular chain displacement (MCD) models to analyze the influence of each variable on breakdown phenomena. The results of this analysis revealed that the amount of space charge accumulation within the insulator has a maximum value at approximately 50 °C, which corresponds to the known morphological transition temperature of LDPE. The breakdown strength calculated using this numerical model was found to decrease with increasing temperature and thickness. Although injection barrier height at the electrode was found to be negatively correlated with breakdown strength, its effect was not as significant as that of the other variables. The breakdown strength values obtained using this numerical method were found to be in close agreement with values reported in the literature. Based on these results, we newly suggest the physical quantity to predict the breakdown strength, the current relaxation speed, which is the slope of the Boltzmann sigmoid function, as a positively correlated index. Finally, we determined that the breakdown phenomena are initiated when the amount of impact accumulated in the insulator changes discontinuously and analyzed the contribution of factors affecting the breakdown using the Pearson correlation coefficient and the Sobol sensitivity index.

INDEX TERMS Bipolar charge transport model, breakdown, finite element method, LDPE, molecular chain displacement model, temperature, thickness.

I. INTRODUCTION

In an HVDC environment, strong uni-directional electric stress applied to the polymeric insulator will generate ionic byproducts that lead to space charge accumulation, which in turn will cause the severe electric field distortion [1], [2]. These physical phenomena will severely reduce the breakdown strength of a polymeric insulator. The breakdown phenomena induced by DC power sources involve a more complicated process than those associated with AC sources [2]–[4]. For polymeric insulators, the mechanism of breakdown is remarkably complicated as a result of the

nonlinear interaction of multiple factors, including the shape and material properties of the electrode, ramp rate, voltage waveform, temperature, thickness, pre-stressing, etc [1], [2], [5]–[11]. This makes it difficult to predict the life expectancy of the insulator or enhance its breakdown strength. Accordingly, developing a better understanding of breakdown mechanism in DC electric devices would be highly useful in enhancing their ability to operate stably with high capacity.

Temperature, thickness, and electrode materials are known to play important roles in determining the breakdown strength of a polymeric insulator. The temperature of an insulator serves to regulate the amount of injected charge, charge carrier mobility, deep trap characteristics, and dynamic characteristics of molecular chains [3], [6], [12].

The associate editor coordinating the review of this manuscript and approving it for publication was Navanietha Krishnaraj Krishnaraj Rathinam.

In contrast, thickness has been shown to be negatively correlated with breakdown strength by Kinzbrunner and Baur [13]. A number of studies have focused on the selection of electrode materials to reduce the space charge injection at the electrode [5], [14]. Each of these factors contributes to the breakdown phenomena of the polymeric insulator in a different manner, making it difficult to analyze their respective effects experimentally. Because the prediction of breakdown strength in terms of all these factors requires statistical analysis involving a large amount of data, it is difficult to distinguish which variables initiate breakdown. In that context, numerical analysis has an advantage in terms of estimating key parameters independently.

Over the past 30 years, numerical analysis has been used as a valuable approach to explain the space charge behavior of polymeric insulators. Alison and Hill suggested the bipolar charge transport (BCT) model, which was further developed by LeRoy in 2004 [15], [16]. Recently, the application of the BCT model to polymeric insulators has been analyzed in terms of various parameters, including the voltage ramp rate, temperature, thickness, and waveform of applied voltage [6], [10], [17]. The molecular chain displacement (MCD) model has also been suggested as a method for explaining the breakdown mechanism at the molecular chain scale [10], [18]–[20]. Until now, however, only a limited range of parameters have been considered, and owing to their nonlinear correlations, few of them have been evaluated.

In this study, the breakdown phenomena of low-density polyethylene (LDPE) were numerically analyzed using a fully-coupled BCT/MCD model based on finite element analysis (FEA). Numerical analysis was carried out with the temperature, and electrode charge injection barrier height, varied and at a wide range of thicknesses from tens of micrometers to millimeters. Using this process, the space charge behavior and current density could be analyzed in real-time. Using a dynamic differential equation, the molecular chain displacement was calculated to determine the initiation of breakdown phenomena. It was found that the breakdown strength decreases with temperature and thickness following a power-law relation and that it decreases slightly as the charge injection barrier height is increased. The breakdown strength calculated using our model is in close agreement with experimental values reported in the literature.

Notably, our findings suggest a new physical quantity to predict the magnitude of breakdown strength based on a simple current density measurement. Under the proposed mechanism, the breakdown strength is positively correlated with the time needed to reach the steady-state current density. Finally, we quantitatively evaluated the effect of temperature, thickness, and injection barrier height on the breakdown strength using the Pearson correlation coefficient and Sobol sensitivity index.

II. THEORETICAL BACKGROUND

To implement the proposed method, we employed two main governing equations, based on the BCT and MCD models,

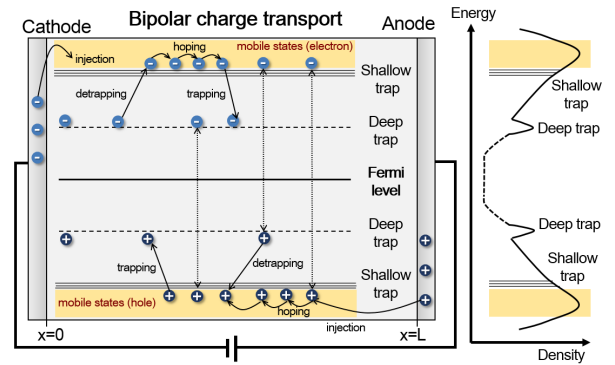


FIGURE 1. (Left) Diagram of BCT model indicating the charge migration process, which involves hopping, trapping, de-trapping, and recombination. (Right) Energy band diagram of a polymeric insulator with shallow and deep traps [24].

respectively. The BCT model was used to analyze the space charge behavior as a function of electric field distribution within the insulator using electrons and holes as charge carriers [18], [21]–[23]. By fully coupling the BCT model and Poisson’s equation, we were able to analyze the distortion in the electric field arising from the space charge distribution. The MCD model was used to explain molecular chain displacement through the use of a dynamic equation incorporating the Coulomb force. This model was used to determine the initiation of breakdown phenomena and breakdown strength.

A. BIPOLAR CHARGE TRANSPORT MODEL

As shown in Fig. 1, the BCT model comprises charge generation and transport processes, including the recombination of oppositely polarized electrons and holes, and the trapping of free mobile charges in a deep trap generated by the chemical defects of the polymeric insulator [23], [25]–[27]. The hopping process, by contrast, is affected by the shallow trap induced by physical defects [28]. Also, it includes the charge injection process at the interface between the electrode and insulator when a strong electric field is applied. These processes are expressed in (1)–(5). Equation (1) expresses the Poisson’s equation for the distribution of space charge density and electric field in the polymeric insulator, (2) is the charge continuity equation, and (3) is the charge transport equation as

$$\nabla \cdot \epsilon_0 \epsilon_r \mathbf{E}(x, t) = \rho_{tot}(x, t) \quad (1)$$

$$\frac{\partial \rho_{tot}}{\partial t}(x, t) + \nabla \cdot \mathbf{J}_c(x, t) = S(x, t) \quad (2)$$

$$\mathbf{J}_c(x, t) = \rho_{free}(x, t) \mu_{e,h} \mathbf{E}(x, t) \quad (3)$$

where ρ_{free} is the free mobile charge density inside the insulator; ρ_{tot} is the total charge density, including the trapped and free charges in C/m^3 ; ϵ_r is the relative permittivity of the insulator; ϵ_0 is the permittivity of vacuum in F/m ; $S(x, t)$ is a reaction term that includes the amount of loss and generation caused by the charge migration, trapping, de-trapping, and recombination; \mathbf{J}_c is the conduction current density arising from the mobile charges in A/m^2 ; $\mu_{e,h}$ is the mobility of

mobile free electrons and holes in $\text{m}^2/\text{V}\cdot\text{s}$; and $\mathbf{E}(x,t)$ is the electric field in V/m .

The mechanism for the charge injection is described in (4) and (5), derived from the Shottky thermionic emission model [29]. This model incorporates the injection barrier height between the electrode and the insulator and the electric field strength at the electrode as

$$J_{in(e)} = AT^2 \exp\left(-\frac{\Phi_{K(e)} - \sqrt{eE(0,t)/4\pi\epsilon_0\epsilon_r}}{K_B T}\right) \quad (4)$$

$$J_{in(h)} = AT^2 \exp\left(-\frac{\Phi_{A(h)} - \sqrt{eE(L,t)/4\pi\epsilon_0\epsilon_r}}{K_B T}\right) \quad (5)$$

where $J_{in(e)}$ and $J_{in(h)}$ are the current densities arising from the injected charge at $x = 0$ (cathode) and $x = L$ (anode), respectively, in A/m^2 ; $\Phi_{K(e)}$ and $\Phi_{A(h)}$ are the injection barrier heights between the electrode and insulator at the cathode and anode, respectively, in eV ; A is the Richardson constant, $1.20 \times 10^6 \text{ A}/\text{m}^2\cdot\text{K}^2$; K_B is the Boltzmann constant; T is the absolute temperature; and e is the unit charge, $1.6 \times 10^{-19} \text{ C}$. The probabilities for trapping and de-trapping are given by

$$P_T = \mu_{e,h} e N_T / \epsilon_0 \epsilon_r \quad (6)$$

$$P_D(E_T) = \nu_{ATE} \exp(-E_T / K_B T) \quad (7)$$

where P_T and P_D are the probabilities of trapping and de-trapping, respectively, in $1/\text{s}$. P_T is proportional to the mobility of the charge carriers, $\mu_{e,h}$, and the deep trap density, N_T , and is inversely proportional to the relative permittivity of the insulator; in the formulation for P_D , ν_{ATE} is the attempt-to-escape frequency in $1/\text{s}$, which is the product of Boltzmann's constant and the temperature divided by Planck's constant written as $K_B T / h$. Following the Langevin model, the probability for recombination between free electrons and free holes is proportional to the sum of their mobilities [30], [31]:

$$\begin{aligned} R_{\mu_e \mu_h} &= \rho_{free(e)} \rho_{free(h)} (\mu_e + \mu_h) / \epsilon_0 \epsilon_r \\ R_{\mu_e t_h} &= \rho_{free(e)} \rho_{trap(h)} \mu_e / \epsilon_0 \epsilon_r \\ R_{t_e \mu_h} &= \rho_{trap(e)} \rho_{free(h)} \mu_h / \epsilon_0 \epsilon_r \end{aligned} \quad (8)$$

where $R_{\mu_e \mu_h}$ is the recombination probability for free electrons and free holes, and $R_{\mu_e t_h}$ and $R_{t_e \mu_h}$ are the recombination probabilities between free and trapped charges, respectively, in $\text{C}/\text{m}^3\cdot\text{s}$. The reaction terms are distinguished by their associated charge types namely, mobile electrons, trapped electrons, mobile holes, and trapped charges. These reaction terms are described as

$$\begin{aligned} S_{\mu_e} &= -P_T(e) \rho_{free(e)} (1 - \rho_{trap(e)} / e N_T(e)) + P_D(e) \rho_{trap(e)} \\ &\quad - R_{\mu_e \mu_h} \rho_{free(e)} \rho_{free(h)} - R_{\mu_e t_h} \rho_{free(e)} \rho_{trap(h)} \\ S_{t_e} &= P_T(e) \rho_{free(e)} (1 - \rho_{trap(e)} / e N_T(e)) - P_D(e) \rho_{trap(e)} \\ &\quad - R_{t_e \mu_h} \rho_{trap(e)} \rho_{free(h)} \\ S_{\mu_h} &= -P_T(h) \rho_{free(h)} (1 - \rho_{trap(h)} / e N_T(h)) + P_D(h) \rho_{trap(h)} \\ &\quad - R_{\mu_e \mu_h} \rho_{free(h)} \rho_{free(e)} - R_{t_e \mu_h} \rho_{free(h)} \rho_{trap(e)} \\ S_{t_h} &= P_T(h) \rho_{free(h)} (1 - \rho_{trap(h)} / e N_T(h)) - P_D(h) \rho_{trap(h)} \\ &\quad - R_{\mu_e t_h} \rho_{trap(e)} \rho_{free(h)} \end{aligned} \quad (9)$$

TABLE 1. Coefficients for BCT model.

Symbol	Quantity	Temperature °C		
		30	50	70
E_T	Deep trap energy (eV)	0.987	1.019	1.072
N_T	Deep trap density $\times 10^{20}$ ($1/\text{eV}\cdot\text{m}^3$)	7.236	5.436	4.934

where the subscripts *trap* and *free* indicate the type of charge carrier and the state, e.g., trapping or de-trapping. To apply the BCT model, it is necessary to determine four representative coefficients: which are the charge injection barrier height between the electrode and insulator, the charge mobilities, and the deep trap energy and density. With the exception of the injection barrier height, which depends on the electrode material, these coefficients vary with temperature. In general, the interval between trapping and de-trapping in the shallow trap is much shorter than the response time of the experimental apparatus [25], [28]. In the numerical model, developed in this study, the mobility at a given temperature was assumed to be constant. As the temperature increases, the electrons and holes pass more rapidly through the insulator, with their respective mobilities varying with temperature as [22]

$$\mu_e(T) = 3.77 \times 10^{-3} \exp(-7529/T) \quad (10)$$

$$\mu_h(T) = 6.84 \times 10^{-4} \exp(-7751/T) \quad (11)$$

where $\mu_e(T)$ and $\mu_h(T)$ are, respectively, the electron and hole mobilities in $\text{m}^2/\text{V}\cdot\text{s}$. It is well understood that the energy and density of the deep trap increase with temperature following the relation depicted in Fig. 2, in which the function on the left represents the shallow density and the function on the right represents the deep trap density as a function of trap level. We analyzed the deep trap distribution by applying the two peaks of a Gaussian function obtained from experimental results in the literature [32]. Figs. 2(a), (b), and (c) show the deep trap energies and density distributions at 30 °C, 50 °C, and 70 °C, respectively. The corresponding deep trap energies and density coefficients applied in the BCT model expressed in (6)-(9) are listed in Table 1.

B. MOLECULAR CHAIN DISPLACEMENT MODEL

The breakdown mechanism in polymeric insulators can be explained in terms of an electro-mechanical process in which the introduction of an electric field causes the displacement of molecular chains due to the Coulomb force. Specifically, the movement of molecular chains is caused by effect of the Coulomb force on the trapped charge in the deep trap. When the displacement of a molecular chain exceeds its threshold length, it begins to deform, following which breakdown is initiated upon the sudden cracking of the insulator. Electrons/holes trapped in the deep trap of the molecular chain are forced to move in opposite to/along the electric field. This process can be explained using the MCD model as

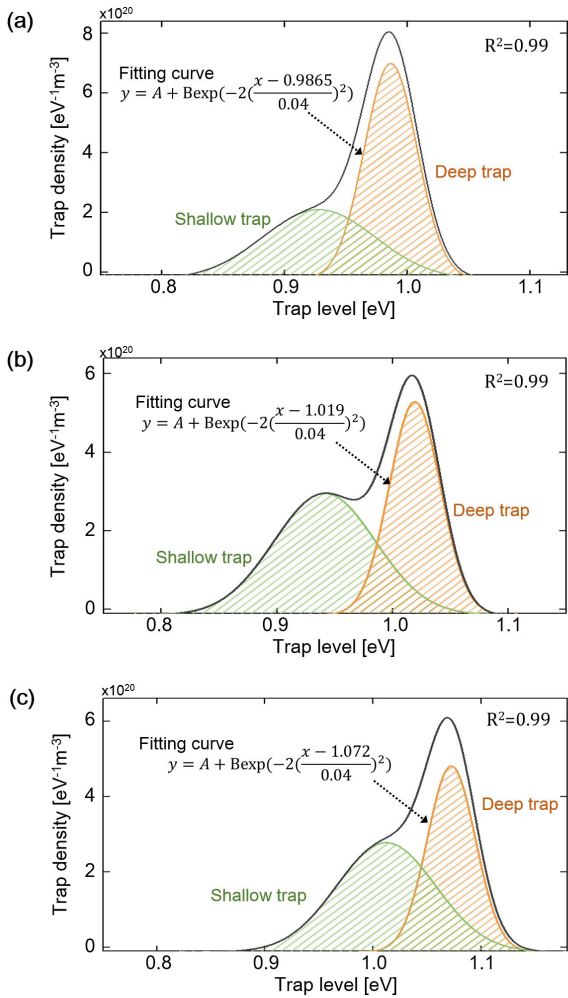


FIGURE 2. Trap energies and density distributions extracted from two peaks of a Gaussian function. The shallow and deep trap energy distributions on the right and left, respectively, correspond to results for (a) 30 °C, (b) 50 °C, and (c) 70 °C. The deep trap energy and density both increase with temperature.

follows [10], [12], [20]:

$$\frac{d\lambda(x, t)}{dt} = \mu_{mol}E(x, t) - \frac{\lambda(x, t)}{\tau_{mol}} \quad (12)$$

where λ is the displacement of the molecular chain in nm, μ_{mol} is the mobility of the molecular chain in $m^2/V \cdot s$, and τ_{mol} is the relaxation time in s. In LDPE, the threshold displacement length for the initiation of breakdown is 23 nm [6].

III. NUMERICAL ANALYSIS MODEL

The numerical model used LDPE as the polymeric insulator with voltage of ramp rate, 400 V/s. Numerical analysis was performed using a fully coupled, one-dimensional BCT/MCD model. In Fig. 1, the positions $x = 0, L$ correspond, respectively, to the locations of the cathode, at which electrons are injected, and the anode, at which holes are injected. The model thickness was varied over a range of with 10–1200 μm and the temperature was changed over the range 30 °C, 50 °C, and 70 °C. To assess the influence of

various electrode materials, the charge injection barrier height was varied over a range of 1.13–1.3 eV [23], [33], [34]. The temperature gradient inside the insulator and the extraction barrier of the electrode were not considered in the model. The extraction barrier in an insulator should be considered when impurity ions are present, as their significant size makes it difficult to escape to the opposite electrode, in which hetero charges should be considered. However, this phenomenon rarely occurs in pure LDPE [33]. The COMSOL Multiphysics commercial software package for FEA was used to simulate the numerical model. As the charge injection was concentrated at the electrode, fine meshes were distributed in its vicinity to improve the numerical stability and accuracy.

IV. NUMERICAL ANALYSIS RESULTS

A. SPACE CHARGE BEHAVIOR

Fig. 3 shows the variation of space charge behavior with temperature within the LDPE at a model thickness of 200 μm . Figs. 3(a), (b), and (c) show the space charge density as a function of time and position x at 30 °C, 50 °C, and 70 °C, respectively. In the figures, the horizontal and vertical axes represent the length in the thickness direction and the time on a logarithmic scale, respectively. At 30 °C, an amount of charge sufficient to distort the electric field begins to inject after $10^{1.8}$ s. At 50 °C and 70 °C, sufficient amounts of charge are injected at earlier times of 16 s and 6 s, respectively. The increase in the voltage applied to both ends of the insulator initially causes the amount of injected charge to increase swiftly, following which it decreases under the influence of the trapped charge. Eventually, the electrical state of the insulator reaches an equilibrium state in terms of the electric field, space charge distribution, and amount of injected charge.

As the temperature increases, the region in which the recombination of holes and electrons occurs actively moves to the cathode from the central region. On the right side of the recombination region, holes are likely to be trapped with high probability, while electrons are trapped actively on the left side. As shown in Fig. 3, the de-trapping process occurs more actively at 50 °C and 70 °C than at 30 °C. Higher temperature reduces the relaxation time needed for the space charge distribution to reach the equilibrium state. At 30 °C, the space charge distribution becomes saturated at approximately 1000 s; at 70 °C, the space charge distribution becomes saturated at around 100 s. At all temperatures, the profiles become quite similar once the space charge distribution has saturated to the steady-state; however, the position at which the polarity of the space charge is reversed differ. The gradient of space charge distribution over the insulator after reaching steady-state is steepest at around 50 °C.

Fig. 4 shows the distributions trapped charge generation and loss density over time, as expressed in (9). The positive values around the anode indicate the generation and loss of trapped holes, while the negative values around the cathode indicate the density of trapped electrons. Figs. 4(a), (b), and (c) show the trapped charge behaviors

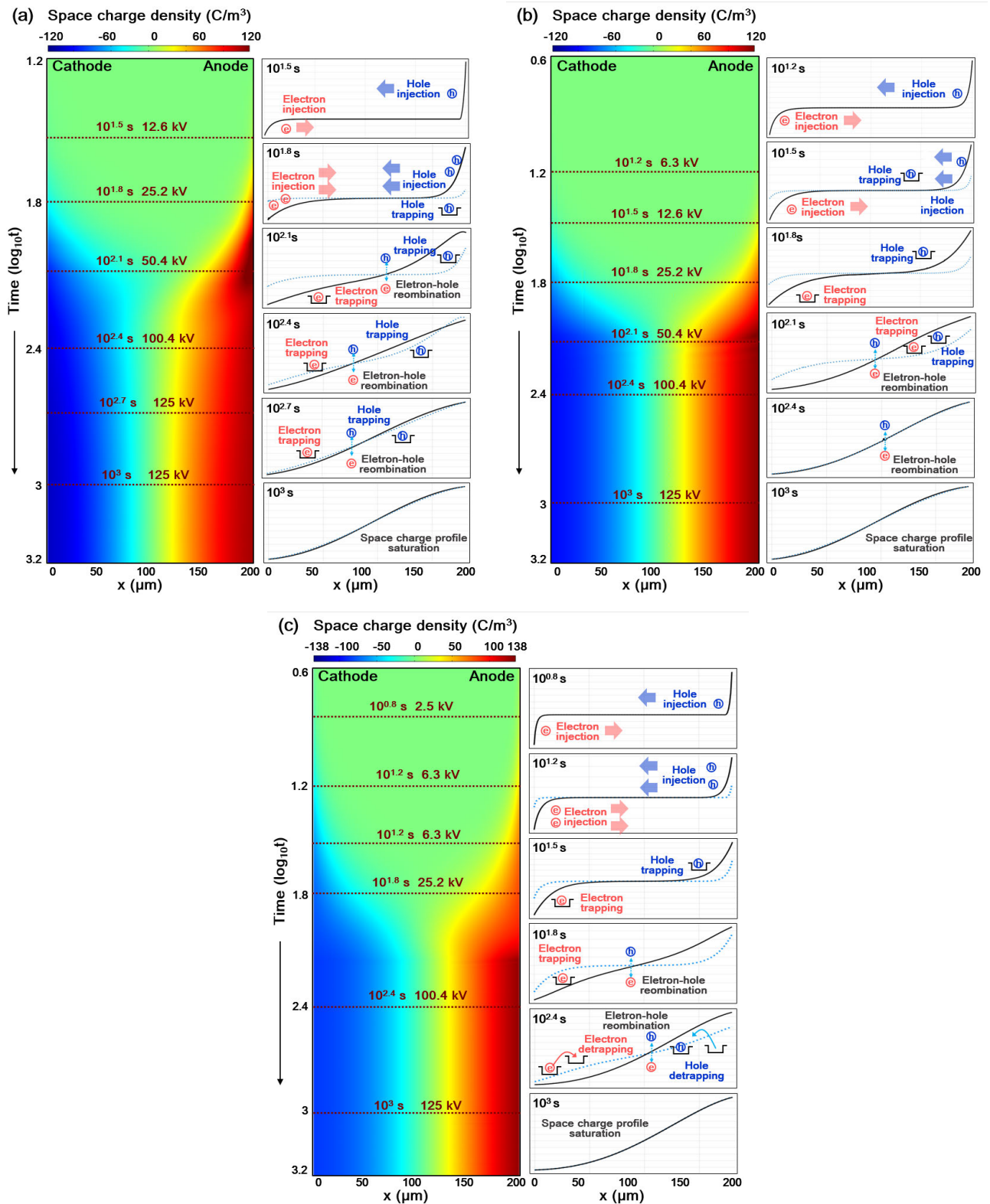


FIGURE 3. Space charge behavior in LDPE as a function of time at a model thickness of $200 \mu m$. The charge accumulation and migration processes clearly differ with temperature. The horizontal and vertical axes represent, respectively, the thickness direction of the LDPE and the log-scale time. Results are shown for (a) $30 \text{ }^\circ C$, (b) $50 \text{ }^\circ C$, and (c) $70 \text{ }^\circ C$.

at $30 \text{ }^\circ C$, $50 \text{ }^\circ C$, and $70 \text{ }^\circ C$, respectively. At $30 \text{ }^\circ C$, a large amount of charge is trapped and accumulated in the

vicinities of the anode and cathode at 100 s, coinciding with the injection tendency of a large amount of charge,

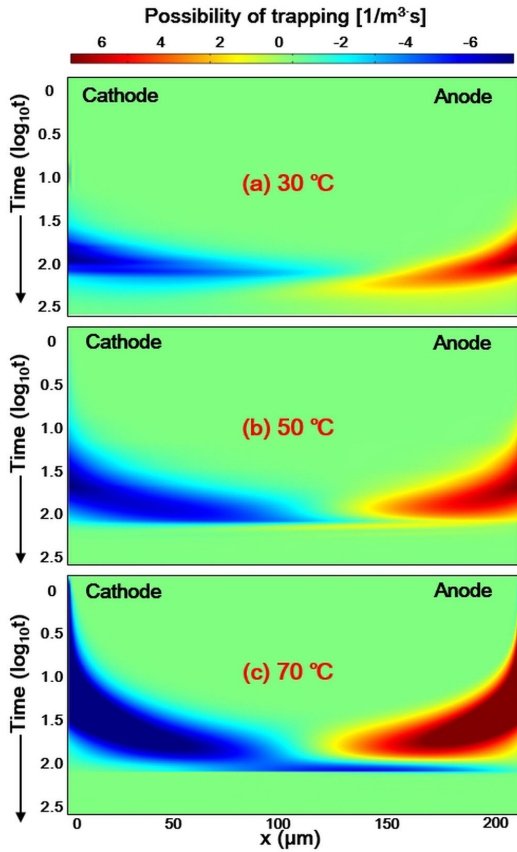


FIGURE 4. Densities of trapped charge generation and loss at (a) 30 °C, (b) 50 °C, and (c) 70 °C. As the temperature increases, the trapped charge increasingly penetrates the central region; at 70 °C, the trapped electrons are found in the vicinity of the anode.

as shown in Fig. 3(a). The presence of trapped charge plays an important role in impeding the charge injection by lowering the electric field strength at the electrode [35]. Initially, the trapped charge is concentrated near the electrode; subsequently, it spreads into the insulator. After sufficient time has passed, the distribution reaches a steady-state.

At 30 °C, both positive and negative charge carriers are trapped near the electrode, causing recombination to occur actively at the center of the insulator. At 50 °C, the probability for trapping increases at both the electrode and the center of the insulator, as shown in Fig. 4(b). Under this condition, charge accumulation by holes, in particular, occurs actively. At 70 °C, high-energy electrons injected from the cathode propagate rapidly and become trapped even in the vicinity of the anode, as shown in Fig. 4(c). The presence of trapped opposite polarity charges near the anode at high temperatures plays a hetero-charge based role in reducing the breakdown strength. Overall, these analysis results help to explain the phenomenon in which the breakdown strength decreases with temperature.

Fig. 5 shows the total amount of accumulated space charge as a function of injection barrier height and temperature. The injection barrier heights at the interface between the electrode and insulator are varied from 1.13 eV to 1.16 eV, 1.2 eV, and,

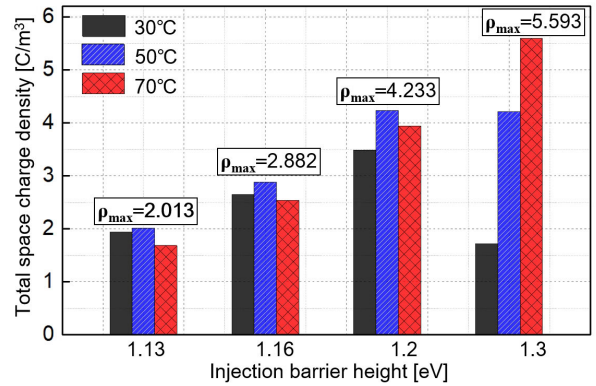


FIGURE 5. Amount of space charge accumulation in LDPE as a function of temperature and injection barrier height. The greatest amount of space charge accumulation occurs at 50 °C except in the 1.3 eV case. These trends are consistent with the literature.

finally, 1.3 eV, while the temperature is varied from 30 °C to 50 °C, and 70 °C. The injected charge is trapped quickly at relatively low temperature, and most of the trapped charges cannot obtain sufficient energy to overcome the deep trap energy needed to become free mobile charges [36]. As shown in Fig. 4(a), however, the injected charge concentrates near the electrode as homo-charge, which forms a local electric field that opposes the applied electric field and reduces the electric field at the interface to interrupt additional charge injection. As a result, a relatively small amount of charge is accumulated inside the insulator.

As the temperature increases, the injection barrier height decreases, enabling the injection of more charge by the electrode. Although more charge can accumulate at 50 °C than at 30 °C, once the temperature exceeds the morphological transition temperature of the LDPE, the movement of charge rapidly accelerates and the probability of hopping into adjacent shallow traps is significantly increased, enhancing the mobility by a factor of 3–4 times. At 70 °C, the space charge accumulation is decreased relative to 50 °C. The occurrence of an inflection temperature at 50 °C agrees well with experimental results reported in the literature [7], [36]–[38]. It reflects a real phenomenon in which the polymer molecular morphology is altered with temperature. However, the inflection point appears only when the injection barrier height between the polymer and electrode is less than 1.3 eV; as shown in Fig. 5, the inflection point disappears at 1.13 eV and a reduced amount of charge is injected into the insulator.

B. CURRENT DENSITY CALCULATION

The total current can be calculated using the average current calculation method [20], [30], [39]:

$$J_{tot} = \frac{1}{L} \int_0^L [J_C + J_D] dx \tag{13}$$

$$J_C(t) = J_h(x, t) + J_e(x, t) \tag{14}$$

$$J_D(x, t) = \epsilon_0 \epsilon_r \frac{\partial D(x, t)}{\partial t} \tag{15}$$

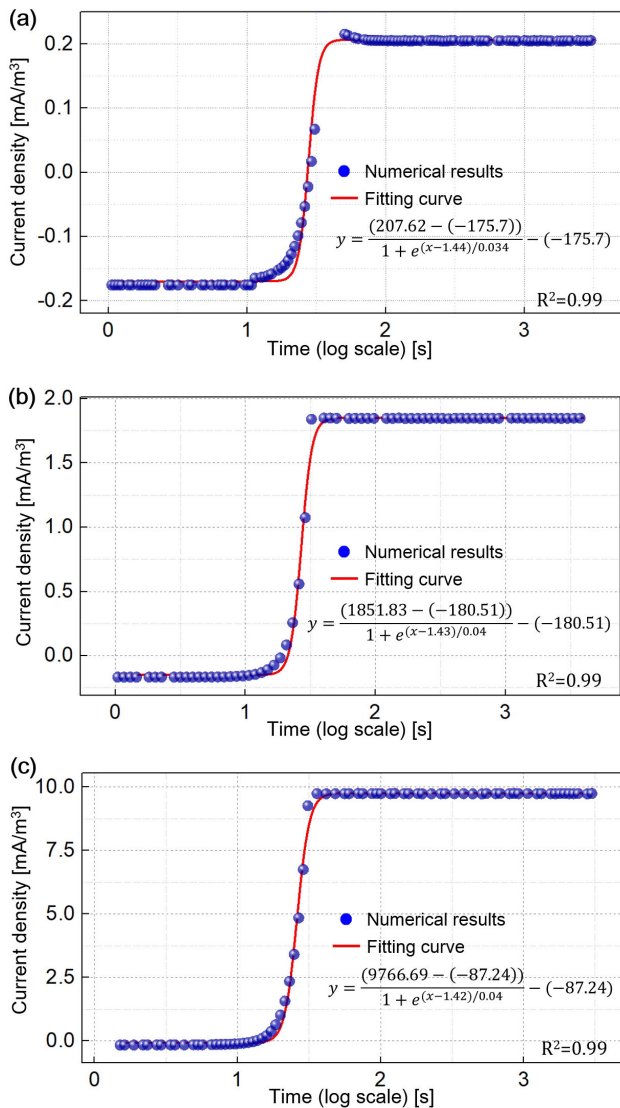


FIGURE 6. Total current densities are passing through LDPE with a thickness of 50 μm and an injection barrier height of 1.2 eV as a function of time (log-scale) at (a) 30 °C, (b) 50 °C, and (c) 70 °C. The current density distributions are fitted to Boltzmann sigmoid functions.

where \mathbf{J}_{tot} is the total current, \mathbf{J}_h is the conduction current caused by the movement of free holes, and \mathbf{J}_e is the conduction current caused by the movement of free electrons. \mathbf{J}_D is the displacement current. To analyze the characteristics of the current calculated using (13), we adopted the Boltzmann sigmoid function as the trend curve, as depicted in Fig 6, and extracted the relevant characteristic parameters to reveal the breakdown characteristics. The general formula of a Boltzmann sigmoid function is expressed as

$$y = \frac{A_1 - A_2}{1 + e^{(x-x_0)/dx}} + A_2 \quad (16)$$

where A_2 and A_1 are the maximum and minimum values, respectively; x_0 is the value of x at which the function has its average value, $(A_1 + A_2)/2$; and dx is the slope at x_0 . Fig. 6 shows the trend curve for (16) as a function of time

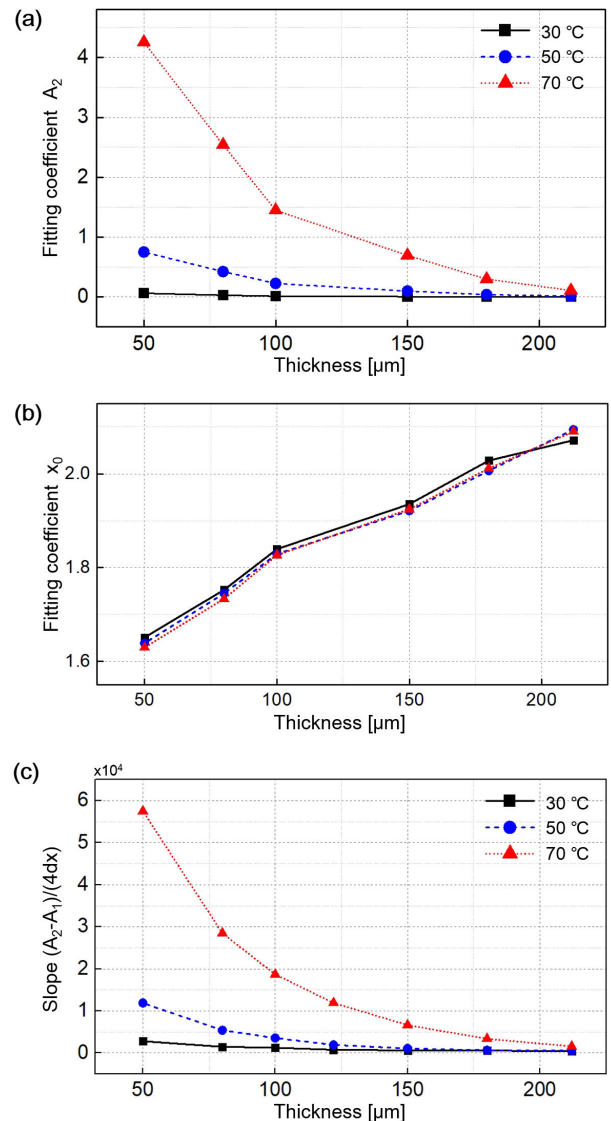


FIGURE 7. Changes in Boltzmann sigmoid function parameters used for fitting of relation between current density and thickness and temperature, showing (a) A_2 , the maximum value of the current density, (b) x_0 , the center coordinate, and (c) slope, $(A_2 - A_1)/4dx$.

at a thickness of 50 μm ; Figs. 6(a), (b), and (c) show the current densities at 30 °C, 50 °C, and 70 °C, respectively. It is seen that the current density distributions all fit closely with a Boltzmann sigmoid function trend.

Fig 7 shows changes in the Boltzmann sigmoid function parameters with thickness and temperature. In Fig. 7(a), the maximum value of the current A_2 decreases and increases with the thickness and temperature, respectively. In Fig. 7(b), by contrast, x_0 increases with thickness but undergoes no noticeable change with temperature. As the thickness increases, the time needed to reach the steady-state current increases. Fig. 7(c) shows the variation of the slope parameter $(A_2 - A_1)/4dx$, an indicator of characteristic speed with which the steady-state current is reached. This parameter can also reflect the electrical relaxation ability of the insulator with thickness and temperature. $(A_2 - A_1)/4dx$

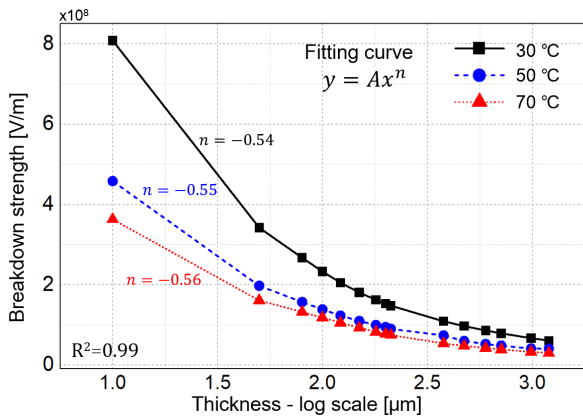


FIGURE 8. Relationship between log-scale thickness and breakdown strength, which follows a temperature-dependent (30 °C, 50 °C, 70 °C) exponential trend curve. The breakdown strength is negatively correlated with temperature and thickness.

decreases and increases with thickness and temperature, respectively.

C. BREAKDOWN STRENGTH PREDICTION WITH CURRENT PROFILE AS CRITICAL INDEX

The breakdown strength is affected by temperature and thickness and related to the electric field distortion caused by the presence of space charge. The initiation of breakdown occurs when the molecular chain displacement reaches the threshold length of 23 nm. Fig. 8 shows the breakdown strength as a function of thickness on a logarithmic scale at a charge injection barrier height of 1.2 eV. The breakdown strength tends to decrease with increasing thickness and temperature. In particular, the relationship between thickness and breakdown strength follows a power law. The index value of -0.5, -0.5, and 0.56 are obtained at 30 °C, 50 °C, and 70 °C, respectively. The exponential relationship between the log scale thickness and the breakdown strength is maintained uniformly at all temperatures, with the inclination of the exponential function becoming steeper as the temperature increases.

The breakdown strength relation calculated from the numerical model developed in this study was validated against results obtained from various references [6], [40], [41]. Fig. 9 shows a comparison of the results obtained from these references and our numerical analysis. In the figure, the circle, triangles, and squares indicate the breakdown strengths at a thickness of 100 μm, and at 1000 V/s, 25 μm at 500 V/s, and 150 μm at 2000 V/s, respectively.

Fig. 10 shows the magnitude of breakdown strength as a function of charge injection barrier height. In Fig. 10(a), in which the LDPE thickness is 10 μm, the highest breakdown strength occurs at 1.13 eV, the lowest charge injection barrier height, across the temperature range. Although the trend varies somewhat depending on the temperature, increasing the charge injection barrier height reduces the breakdown strength. In the thin film-type insulator, as shown in Fig. 10(a), the high charge injection barrier height hinders the charge injection process, intensifying the electric field

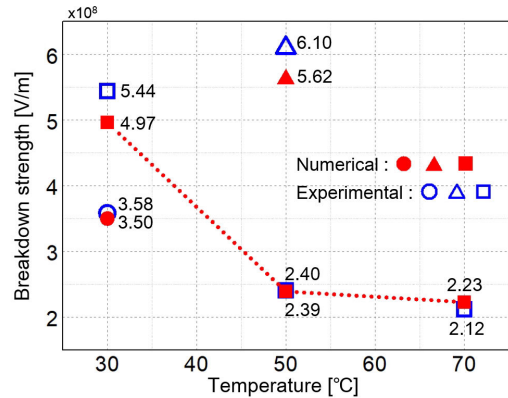


FIGURE 9. Comparison between numerical analysis results and experimental results obtained from [6], [40], [41].

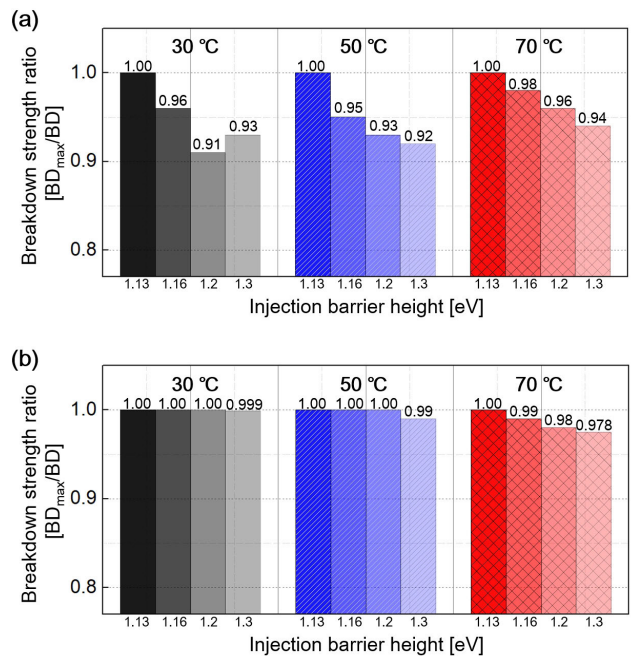


FIGURE 10. Comparison of the relative magnitudes of breakdown strengths with different injection barrier heights at 30 °C, 50 °C, and 70 °C. Results are obtained at thickness of (a) 10 μm and (b) 180 μm. In most cases, the strongest breakdown strength occurs at 1.13 eV.

distortion and reducing the breakdown strength. Fig. 10(b) shows the relative breakdown strengths at a thickness of 180 μm as a function of temperature and charge injection barrier height. As the thickness increases, the effect of the charge injection barrier height decreases steeply, especially at the low temperature range of 30 °C and 50 °C. As shown in Figs. 10(a) and (b), at 70 °C the charge injection barrier height is higher, the breakdown strength is reduced regardless of thickness. As these results reveal, parameters such as temperature, thickness, injection barrier height jointly affect the breakdown strength in a nonlinear manner.

Based on the analysis results in this study, we propose a new physical quantity, the speed parameter $(A_2 - A_1)/4dx$, as an indicator for predicting the breakdown strength. The speed parameter corresponds to the rapidity with which the

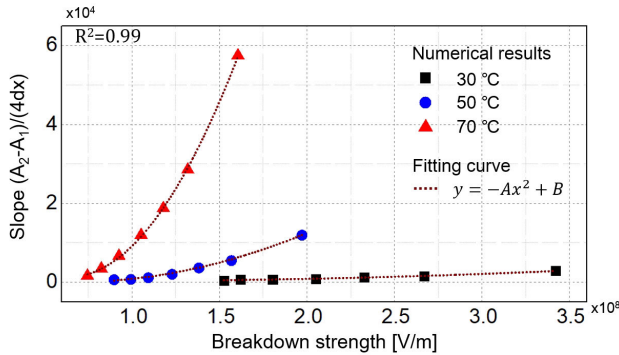


FIGURE 11. Plots showing quadratic relation between the slope parameter of the Boltzmann sigmoid function and the breakdown strength at temperature of 30 °C, 50 °C, and 70 °C.

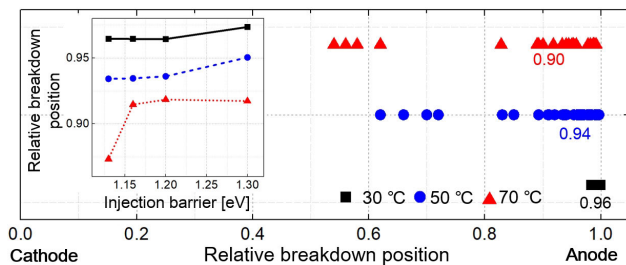


FIGURE 12. Breakdown positions depicted as relative locations within an insulator in which the cathode and anode are located at $x = 0, 1$, respectively. As temperature increases, the breakdown position moves from the vicinity of the electrode to the central region of the LDPE.

steady-state current density is achieved and takes the form of a Boltzmann sigmoid function, as shown in Fig. 7(c). Increasing the local electric field distortion within the insulator results in the accumulation of a large amount of space charge with high kinetic energy, which in turns weakens the breakdown strength. If there are sufficient amount and speed of charge to relieve the local electric field distortion in the insulator, the breakdown strength can be enhanced. As shown in Fig. 11, the relationship between the speed parameter $(A_2 - A_1)/4dx$, and breakdown strength can be expressed as a quadratic function for which the slope steepens as the temperature increases. This relation indicates that the current relaxation ability in the insulator acts as a critical parameter for the breakdown strength at high temperatures. In this context, the breakdown strength of polymeric insulators can be deduced from the real-time current profile passing through the insulator. In particular, the speed parameter reaching the steady-state plays an important role as a critical index that can predict the strength of insulation breakdown.

D. BREAKDOWN POSITION

Fig. 12 shows the relative positions at which breakdown occurs in the insulator as a function of temperature. These points indicate where the molecular chain displacement length exceeds 23 nm as well as where the electric field strength has a maximum magnitude and the polarity of space charge is reversed as a result of the active recombination of charge carriers. Fig. 12 shows the locations of breakdown

in all cases within the thickness range of 10–1200 μm , at temperatures of 30 °C, 50 °C, and 70 °C, and at barrier heights of 1.13–1.3 eV. At 30 °C, 50 °C, and 70 °C, breakdown occurs at relative positions within the insulator of 0.96, 0.94, and 0.90, respectively, indicating that, as the temperature increases, the breakdown position moves toward the center of the insulator. Unlike electrons, which quickly pass through the insulator, the number of injected holes, which play an essential role in the electric field distortion, increases considerably with temperature. As a result, the location at which recombination occurs moves away from the anode and toward the center of the insulator. Furthermore, regardless of the charge injection barrier height, the breakdown occurs at the farthest distance from the electrode at 70 °C.

The initiation of the breakdown phenomenon is determined by sever molecular chain displacement, as expressed in (12). In our preceding study, the mechanical stress caused by molecular chain displacement was explained using a physical approach in terms of the momentum-impact relation [24]. For a given same magnitude of electric force, the amount of impact stored in a molecular chain will vary with the time at which the electric force acts. The change in the momentum of the molecular chain will increase with the amount of impact. The breakdown position will be located at the position at which the amount of impact accumulated in the insulator changes discontinuously. This sudden discontinuous impact will cause a locally intensive electro-mechanical stress within the insulator, which in turn will have a destructive internal impact leading to the breakdown. The distribution of accumulative impact in an insulator can be expressed as an integral over time of the electric force acting on the trapped charge at the molecular chain:

$$I_p(x, t) = \int_0^t (\rho_{\text{trap}(h)}(x, t_0) - \rho_{\text{trap}(e)}(x, t_0)) \mathbf{E}(x, t_0) dt_0 \quad (17)$$

where $I_p(x, t)$ is the amount of impact accumulated at position x on the insulator, $\rho_{\text{trap}(h)}$ is the charge density of holes trapped in the deep trap, $\rho_{\text{trap}(e)}$ is the charge density of trapped electrons, and $\mathbf{E}(x, t_0)$ is the electric field at time t_0 at insulator position x . To cause a breakdown within the insulator, the space charge should have enough energy to pull the molecular chain displacement to a critical length. Furthermore, because the electrical stress is locally concentrated at the position at which the impact accumulates, a discontinuous change in momentum will occur to initiate the breakdown. Fig. 13 shows the distributions of the accumulated impact within the molecular chain and breakdown location at various temperature. In each case, the position, at which discontinuous momentum change occurs as a result of a sudden increase in the amount of impact coincides with the breakdown position.

V. DISCUSSION

We quantitatively evaluate a number of parameters, including voltage ramp rate, thickness, temperature, and injection barrier height, as shown in Fig. 14. The Pearson correlation

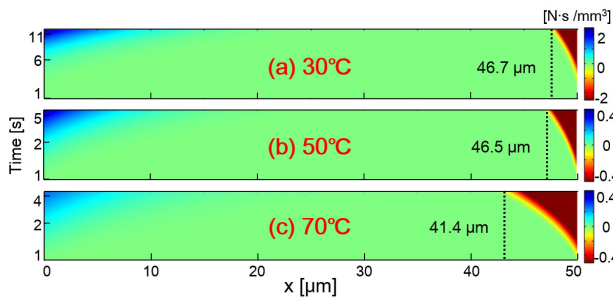


FIGURE 13. Change in cumulative impact distributions over time in LDPE thickness of 50 μm . Breakdown occurs at the position at which the cumulative impulse changes suddenly. At (a) 30 $^{\circ}\text{C}$, the breakdown position is at 46.7 μm . At (b) 50 $^{\circ}\text{C}$, the breakdown position is at 46.5 μm . At (c) 70 $^{\circ}\text{C}$, the breakdown position is at 41.4 μm .

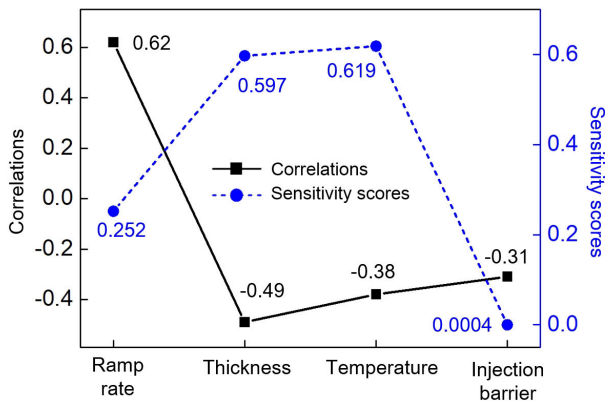


FIGURE 14. Estimation of the effects of the voltage ramp rate, thickness, temperature, and injection barrier height on breakdown strength using Pearson correlation index and Sobol sensitivity value.

and Sobol sensitivity index were used to analyze 168 cases, including our previous research [24]. Thickness, temperature, and charge injection barrier height were found to have a negative correlation with breakdown strength, while a voltage ramp rate was found to be positively correlated with breakdown strength. The Sobol sensitivity index results revealed the degree to which each variable affects the breakdown strength based on an application of a variance-based analysis method in which each parameter is assumed to be independent [42]. From this analysis, parameters related to breakdown strength are, in order of importance, temperature, thickness, and voltage ramp rate.

VI. CONCLUSION

In this study, we analyzed the breakdown phenomena occurring in LDPE by varying several parameters. Specifically, we numerically analyzed the breakdown phenomena at injection barrier heights in the range of 1.13–1.3 eV, insulator thickness in the range of 10–1200 μm , and temperature in the range of 30–70 $^{\circ}\text{C}$. To carry out the BCT and the MCD models were fully coupled employing the FEA. The space charge behavior and trends in breakdown strength at various parameter settings were both found to be in close agreement with experimental results from the literature, thereby validating the proposed numerical model.

Except in the case in which the injection barrier was 1.3 eV, the maximum amount of space charges is accumulated in the LDPE occurred at 50 $^{\circ}\text{C}$. This numerical result closely reflects the relation between the transition temperature of the LDPE and the space charge accumulation. It was also shown that the breakdown strength followed a power-law relationship with the logarithmic thickness of the LDPE, with the steepness of the exponential relation increasing at higher temperatures. By contrast, the thickness and temperature were found to be negatively correlated with the breakdown strength. To predict the breakdown strength, we proposed the speed parameter as a physical indicator of the rapidity with which the steady-state current density is reached. This parameter is adapted from the Boltzmann sigmoid function and has a positive correlation with breakdown strength. Based on the speed parameter, we concluded that an important factor in determining the breakdown strength is the ability to mitigate the local energy imbalance in the insulator. Also, the breakdown occurs at the position at which the local energy imbalance is intensified.

Finally, we evaluated the various parameters that affect the breakdown strength using Pearson's correlation coefficient and the Sobol sensitivity method. The voltage ramp rate was found to be positively correlated with breakdown strength, whereas temperature, thickness, and charge injection barrier height were found to be negatively correlated with the breakdown strength. Among these parameters, temperature was found to have the most significant influence on the breakdown strength of the insulator.

The results of this study suggest the possibility of developing a method for predicting breakdown strength by quantitatively evaluating the influence of various parameters employing the proposed numerical analysis model. As a new systematic technique for analyzing the breakdown phenomena, this numerical approach can be applied as an optimization tool for improving the insulation performance of electrical equipment.

REFERENCES

- [1] T. Mizutani, H. Semi, and K. Kaneko, "Space charge behavior in low-density polyethylene," *IEEE Trans. Dielectr. Electr. Insul.*, vol. 7, no. 4, pp. 503–508, Aug. 2000, doi: [10.1109/94.868069](https://doi.org/10.1109/94.868069).
- [2] D. Fabiani, G. C. Montanari, C. Laurent, G. Teyssedre, P. H. F. Morshuis, R. Bodega, L. A. Dissado, A. Campus, and U. H. Nilsson, "Polymeric HVDC cable design and space charge Accumulation. Part 1: Insulation/Semicon interface," *IEEE Elect. Insul. Mag.*, vol. 23, no. 6, pp. 11–19, Nov. 2007, doi: [10.1109/MEI.2007.4389975](https://doi.org/10.1109/MEI.2007.4389975).
- [3] Z. Li, M. Fan, Z. Zhong, and B. Du, "Coupling effect of molecular chain displacement and carrier trap characteristics on DC breakdown of HDPE/LDPE blend insulation," *Polymers*, vol. 12, no. 3, p. 589, Mar. 2020, doi: [10.3390/polym12030589](https://doi.org/10.3390/polym12030589).
- [4] W. Yin and D. Schweickart, "Dielectric breakdown of polymeric insulation films under AC, DC and pulsed voltages," in *Proc. IEEE Electr. Insul. Conf.*, May 2009, pp. 292–296.
- [5] K. Miyairi and T. Yamada, "High field conduction current and electric breakdown in polyethylene," *Jpn. J. Appl. Phys.*, vol. 16, no. 8, pp. 1449–1450, Aug. 1977, doi: [10.1143/JJAP.16.1449](https://doi.org/10.1143/JJAP.16.1449).
- [6] D. Min, S. Li, and Y. Ohki, "Numerical simulation on molecular displacement and DC breakdown of LDPE," *IEEE Trans. Dielectr. Electr. Insul.*, vol. 23, no. 1, pp. 507–516, Feb. 2016, doi: [10.1109/TDEI.2015.005402](https://doi.org/10.1109/TDEI.2015.005402).

- [7] M. Ieda, "Dielectric breakdown process of polymers," *IEEE Trans. Electr. Insul.*, vols. EI-15, no. 3, pp. 206–224, Jun. 1980, doi: [10.1109/TEI.1980.298314](https://doi.org/10.1109/TEI.1980.298314).
- [8] S. Wang, S. Yu, J. Xiang, J. Li, and S. Li, "DC breakdown strength of crosslinked polyethylene based nanocomposites at different temperatures," *IEEE Trans. Dielectrics Electr. Insul.*, vol. 27, no. 2, pp. 482–488, Apr. 2020, doi: [10.1109/TDEI.2019.008572](https://doi.org/10.1109/TDEI.2019.008572).
- [9] L. Cao, L. Zhong, Y. Li, Z. Shen, L. Jiang, J. Gao, and G. Chen, "Effect of blend of polystyrene on the temperature dependence of DC breakdown characteristics of polyethylene," in *Proc. Condition Monitor. Diagnosis (CMD)*, Sep. 2018, pp. 1–4.
- [10] D. Min, Y. Li, C. Yan, D. Xie, S. Li, Q. Wu, and Z. Xing, "Thickness-dependent DC electrical breakdown of polyimide modulated by charge transport and molecular displacement," *Polymers*, vol. 10, no. 9, p. 1012, Sep. 2018, doi: [10.3390/polym10091012](https://doi.org/10.3390/polym10091012).
- [11] G. Chen, J. Zhao, S. Li, and L. Zhong, "Origin of thickness dependent DC electrical breakdown in dielectrics," *Appl. Phys. Lett.*, vol. 100, no. 22, May 2012, Art. no. 222904, doi: [10.1063/1.4721809](https://doi.org/10.1063/1.4721809).
- [12] J. Lowell, "Absorption and conduction currents in polymers: A unified model," *J. Phys. D, Appl. Phys.*, vol. 23, no. 2, pp. 205–210, Feb. 1990, doi: [10.1088/0022-3727/23/2/011](https://doi.org/10.1088/0022-3727/23/2/011).
- [13] J. O. Kraehenbuehl and C. W. Parmelee, "A study of the electrical strength of porcelain," *Trans. Electrochem. Soc.*, vol. 59, no. 1, p. 53, 1931, doi: [10.1149/1.3497836](https://doi.org/10.1149/1.3497836).
- [14] M. Taleb, G. Teysse, and S. Le Roy, "Role of the interface on charge build-up in a low-density polyethylene: Surface roughness and nature of the electrode," in *Proc. IEEE Conf. Electr. Insul. Dielectr. Phenomena*, Aug. 2009, pp. 112–115.
- [15] J. M. Alison and R. M. Hill, "A model for bipolar charge transport, trapping and recombination in degassed crosslinked polyethene," *J. Phys. D, Appl. Phys.*, vol. 27, no. 6, pp. 1291–1299, Jun. 1994, doi: [10.1088/0022-3727/27/6/029](https://doi.org/10.1088/0022-3727/27/6/029).
- [16] S. Le Roy, G. Teysse, P. Segur, and C. Laurent, "Modelling of space charge, electroluminescence and current in low density polyethylene under DC and AC field," in *Proc. 17th Annu. Meeting IEEE Lasers Electro-Optics Soc.*, 2004, pp. 29–32.
- [17] D. Min, W. Wang, and S. Li, "Numerical analysis of space charge accumulation and conduction properties in LDPE nanodielectrics," *IEEE Trans. Dielectr. Electr. Insul.*, vol. 22, no. 3, pp. 1483–1491, Jun. 2015, doi: [10.1109/TDEI.2015.7116341](https://doi.org/10.1109/TDEI.2015.7116341).
- [18] D. Min, H. Cui, W. Wang, Q. Wu, Z. Xing, and S. Li, "The coupling effect of interfacial traps and molecular motion on the electrical breakdown in polyethylene nanocomposites," *Compos. Sci. Technol.*, vol. 184, Nov. 2019, Art. no. 107873, doi: [10.1016/j.compscitech.2019.107873](https://doi.org/10.1016/j.compscitech.2019.107873).
- [19] Y. Li, "Numerical simulation on DC breakdown of polyimide based on charge transport and molecular chain displacement," in *Proc. 21st Int. Symp. High Voltage Eng.*, vol. 598, 2020, pp. 108–117.
- [20] S. Li, D. Min, W. Wang, and G. Chen, "Modelling of dielectric breakdown through charge dynamics for polymer nanocomposites," *IEEE Trans. Dielectr. Electr. Insul.*, vol. 23, no. 6, pp. 3476–3485, Dec. 2016, doi: [10.1109/TDEI.2016.006051](https://doi.org/10.1109/TDEI.2016.006051).
- [21] F. Boufayed, "Models of bipolar charge transport in polyethylene," *J. Appl. Phys.*, vol. 100, no. 10, 2006, Art. no. 104105, doi: [10.1063/1.2375010](https://doi.org/10.1063/1.2375010).
- [22] S. Zhang and Y. Liu, "Simulation of space charge accumulation in LDPE under temperature gradient with temperature-dependent parameters," in *Proc. IEEE Int. Conf. Properties Appl. Dielectr. Mater.*, May 2018, 2018, pp. 1028–1032.
- [23] S. L. Roy, P. Segur, G. Teysse, and C. Laurent, "Description of bipolar charge transport in polyethylene using a fluid model with a constant mobility: Model prediction," *J. Phys. D, Appl. Phys.*, vol. 37, no. 2, pp. 298–305, Jan. 2004, doi: [10.1088/0022-3727/37/2/020](https://doi.org/10.1088/0022-3727/37/2/020).
- [24] M. Kim, S.-H. Kim, and S.-H. Lee, "Finite element analysis of the breakdown prediction for LDPE stressed by various ramp rates of DC voltage based on molecular displacement model," *Energies*, vol. 13, no. 6, p. 1320, Mar. 2020, doi: [10.3390/en13061320](https://doi.org/10.3390/en13061320).
- [25] M. Meunier and N. Quirke, "Molecular modeling of electron trapping in polymer insulators," *J. Chem. Phys.*, vol. 113, no. 1, pp. 369–376, Jul. 2000, doi: [10.1063/1.481802](https://doi.org/10.1063/1.481802).
- [26] M. Meunier, N. Quirke, and A. Aslanides, "Molecular modeling of electron traps in polymer insulators: Chemical defects and impurities," *J. Chem. Phys.*, vol. 115, no. 6, pp. 2876–2881, Aug. 2001, doi: [10.1063/1.1385160](https://doi.org/10.1063/1.1385160).
- [27] T.-C. Zhou, G. Chen, R.-J. Liao, and Z. Xu, "Charge trapping and detrapping in polymeric materials: Trapping parameters," *J. Appl. Phys.*, vol. 110, no. 4, Aug. 2011, Art. no. 043724, doi: [10.1063/1.3626468](https://doi.org/10.1063/1.3626468).
- [28] S. Li, D. Min, W. Wang, and G. Chen, "Linking traps to dielectric breakdown through charge dynamics for polymer nanocomposites," *IEEE Trans. Dielectr. Electr. Insul.*, vol. 23, no. 5, pp. 2777–2785, Oct. 2016, doi: [10.1109/TDEI.2016.7736837](https://doi.org/10.1109/TDEI.2016.7736837).
- [29] F. Baudoin, S. Le Roy, G. Teysse, and C. Laurent, "Bipolar charge transport model with trapping and recombination: An analysis of the current versus applied electric field characteristic in steady state conditions," *J. Phys. D, Appl. Phys.*, vol. 41, no. 2, Jan. 2008, Art. no. 025306, doi: [10.1088/0022-3727/41/2/025306](https://doi.org/10.1088/0022-3727/41/2/025306).
- [30] A. C. Kusumasebada, G. Teysse, S. Le Roy, L. Boudou, and N. I. Sinsuka, "Assessment of a charge transport model for LDPE through conduction current measurement," *Adv. Technol. Innov.*, vol. 2, no. 1, p. 1, Jan. 2017.
- [31] S. L. Roy, G. Teysse, and C. Laurent, "Modelling space charge in a cable geometry," *IEEE Trans. Dielectr. Electr. Insul.*, vol. 23, no. 4, pp. 2361–2367, Aug. 2016, doi: [10.1109/TDEI.2016.7556514](https://doi.org/10.1109/TDEI.2016.7556514).
- [32] L. Zhao, G.-Z. Liu, J.-C. Su, Y.-F. Pan, and X.-B. Zhang, "Investigation of thickness effect on electric breakdown strength of polymers under nanosecond pulses," *IEEE Trans. Plasma Sci.*, vol. 39, no. 7, pp. 1613–1618, Jul. 2011, doi: [10.1109/TPS.2011.2143435](https://doi.org/10.1109/TPS.2011.2143435).
- [33] G. Teysse and C. Laurent, "Charge transport modeling in insulating polymers: From molecular to macroscopic scale," in *IEEE Trans. Dielectr. Electr. Insul.*, vol. 2005, no. 5, pp. 857–874, doi: [10.1109/TDEI.2005.1522182](https://doi.org/10.1109/TDEI.2005.1522182).
- [34] K. Kaneko, T. Mizutani, and Y. Suzuoki, "Computer simulation on formation of space charge packets in XLPE films," *IEEE Trans. Dielectr. Electr. Insul.*, vol. 6, no. 2, pp. 152–158, Apr. 1999, doi: [10.1109/94.765904](https://doi.org/10.1109/94.765904).
- [35] Z. Li, B. Du, C. Han, and H. Xu, "Trap modulated charge carrier transport in polyethylene/graphene nanocomposites," *Sci. Rep.*, vol. 7, no. 1, Dec. 2017, Art. no. 4015, doi: [10.1038/s41598-017-04196-5](https://doi.org/10.1038/s41598-017-04196-5).
- [36] G. Li, X. Zhou, C. Hao, Q. Lei, and Y. Wei, "Temperature and electric field dependence of charge conduction and accumulation in XLPE based on polarization and depolarization current," *AIP Adv.*, vol. 9, no. 1, Jan. 2019, Art. no. 015109, doi: [10.1063/1.5064413](https://doi.org/10.1063/1.5064413).
- [37] L. Boudou and J. Guastavino, "Influence of temperature on low-density polyethylene films through conduction measurement," *J. Phys. D, Appl. Phys.*, vol. 35, no. 13, pp. 1555–1561, Jul. 2002, doi: [10.1088/0022-3727/35/13/317](https://doi.org/10.1088/0022-3727/35/13/317).
- [38] G. Li, J. Wang, W. Han, Y. Wei, and S. Li, "Influence of temperature on charge accumulation in low-density polyethylene based on depolarization current and space charge decay," *Polymers*, vol. 11, no. 4, p. 587, Apr. 2019, doi: [10.3390/polym11040587](https://doi.org/10.3390/polym11040587).
- [39] A. Hoang, Y. Serdyuk, and S. Gubanski, "Charge transport in LDPE nanocomposites part II—Computational approach," *Polymers*, vol. 8, no. 4, p. 103, Mar. 2016, doi: [10.3390/polym8040103](https://doi.org/10.3390/polym8040103).
- [40] S. Song, H. Zhao, Z. Yao, Z. Yan, J. Yang, X. Wang, and X. Zhao, "Enhanced electrical properties of Polyethylene-Graft-Polystyrene/LDPE composites," *Polymers*, vol. 12, no. 1, p. 124, Jan. 2020, doi: [10.3390/polym12010124](https://doi.org/10.3390/polym12010124).
- [41] K. Wu, X. Chen, X. Liu, X. Wang, Y. Cheng, and L. A. Dissado, "Study of the space charge behavior in polyethylene nano-composites under temperature gradient," in *Proc. Int. Symp. Electr. Insulating Mater.*, Sep. 2011, pp. 84–87.
- [42] I. M. Sobol and S. S. Kucherenko, "Global sensitivity indices for nonlinear mathematical models. Review," *Wilmott*, vol. 2005, no. 1, pp. 56–61, Jan. 2005, doi: [10.1002/wilm.42820050114](https://doi.org/10.1002/wilm.42820050114).



MINHEE KIM received the B.S. degree in physics from Sungkyunkwan University, Suwon, South Korea, in 2012, and the M.S. degree in electrical engineering from Kyungpook National University, Daegu, South Korea, in 2019, where she is currently pursuing the Ph.D. degree. Her research interests include breakdown, high voltage, electric discharge, space charge dynamics, polymeric insulators, and interface phenomena at hetero-dielectric insulators.



SU-HUN KIM (Member, IEEE) received the B.S. degree from the Department of Electronic Engineering, Paichai University, Daejeon, South Korea, in 2012, and the M.S. degree from the Department of Energy Science, Sungkyunkwan University, Suwon, South Korea, in 2014. He is currently pursuing the Ph.D. degree with the Department of Electrical Engineering, Kyungpook National University, Daegu, South Korea. His research interests include superconductivity, high magnetic field, cryogenic, electromagnetic multiphysics system designs, electric discharge, high voltage, electromagnet, energy harvesting, and nano devices.



SE-HEE LEE received the B.S. and M.S. degrees in electrical engineering from Soongsil University, Seoul, South Korea, in 1996 and 1998, respectively, and the Ph.D. degree in electrical and computer engineering from Sungkyunkwan University, Suwon, South Korea, in 2002. He was a Postdoctoral Researcher with the Massachusetts Institute of Technology (MIT). He joined the Department of Electrical Engineering, Faculty of Kyungpook National University, in 2008. He worked with the Korea Electrotechnology Research Institute (KERI). His research interests include analysis and design for electromagnetic multiphysics problems spanning the macro- to the nano-scales.

...